Scientific Reports

https://doi.org/10.1038/s41598-026-38583-8

Article in Press

Mesoporous silicon microparticles enhance antiviral immunity and memory responses against SARS-CoV-2

Received: 3 September 2025

Accepted: 30 January 2026

Published online: 05 February 2026

Cite this article as: López-Gómez A., Real-Arévalo I., Mayol-Hornero E. *et al.* Mesoporous silicon microparticles enhance antiviral immunity and memory responses against SARS-CoV-2. *Sci Rep* (2026). https://doi.org/10.1038/s41598-026-38583-8

Ana López-Gómez, Irene Real-Arévalo, Elsa Mayol-Hornero, Jana Ausio Cendra, Diego Laxalde-Fernández, Pablo Nogales-Altozano, Benigno Rivas-Pardo, Beatriz Amorós-Pérez, Beatriz Martín-Adrados, Ignacio Juárez, Álvaro Martínez-Del-Pozo, Raúl J. Martín-Palma, Noemí Sevilla, Eduardo Martínez-Naves & Manuel Gómez Moral

We are providing an unedited version of this manuscript to give early access to its findings. Before final publication, the manuscript will undergo further editing. Please note there may be errors present which affect the content, and all legal disclaimers apply.

If this paper is publishing under a Transparent Peer Review model then Peer Review reports will publish with the final article.

ARTICLE IN PRESS

© The Author(s) 2026. **Open Access** This article is licensed under a Creative Commons Attribution-NonCommercial-NoDerivatives 4.0 International License, which permits any non-commercial use, sharing, distribution and reproduction in any medium or format, as long as you give appropriate credit to the original author(s) and the source, provide a link to the Creative Commons licence, and indicate if you modified the licensed material. You do not have permission under this licence to share adapted material derived from this article or parts of it. The images or other third party material in this article are included in the article's Creative Commons licence, unless indicated otherwise in a credit line to the material. If material is not included in the article's Creative Commons licence and your intended use is not permitted by statutory regulation or exceeds the permitted use, you will need to obtain permission directly from the copyright holder. To view a copy of this licence, visit http://creativecommons.org/licenses/by-nc-nd/4.0/.

ARTICLE IN PRESS

TITLE: **Mesoporous silicon microparticles enhance antiviral immunity and memory responses against SARS-CoV-2**

Ana López-Gómez[1,2], Irene Real-Arévalo[2,3], Elsa Mayol-Hornero[1,2], Jana Ausio Cendra[1], Diego Laxalde-Fernández[4], Pablo Nogales-Altozano[6], Benigno Rivas-Pardo[2], Beatriz Amorós-Pérez[2,3], Beatriz Martín-Adrados[2], Ignacio Juárez[2], Álvaro Martínez-Del-Pozo[4], Raúl J. Martín-Palma[5], Noemí Sevilla[6], Eduardo Martínez-Naves[2*], Manuel Gómez del Moral[1*]

[1] Department of Cellular Biology and Histology, School of Medicine, Universidad Complutense of Madrid (UCM), 28040 Madrid, Spain

[2] Department of Immunology, Ophthalmology and ORL, School of Medicine, Universidad Complutense of Madrid (UCM), 28040 Madrid, Spain

[3] Inmunotek S.L., 28805 Alcalá de Henares, Spain

[4] Department of Biochemistry and Molecular Biology, School of Chemistry, Universidad Complutense of Madrid, 28040 Madrid, Spain.

[5] Department of applied physics, Universidad Autónoma de Madrid, Madrid, España

[6] Centro de Investigación en Sanidad Animal, Instituto Nacional de Investigación y Tecnología Agraria y Alimentaria, Consejo Superior de Investigaciones Científicas (CISA-INIA-CSIC), Valdeolmos, Madrid, Spain

*EMN and MGM contributed equally to this work

Corresponding Authors: EMN; emnaves@ucm.es; MGM; mgomezm@ucm.es

ARTICLE IN PRESS

Fundings:

This work was supported by grants from Comunidad de Madrid (COV20/01101-CM and REACT-UE, ANTICIPA-CM Ref. PR38/21-24) to E.M.N and M.G.M and from Spanish Ministry of Science and Innovation (RETOS PID2022-1366620B-100) to M.G.M.

Abstract:

Silica-based materials have attracted considerable interest as vaccine adjuvants due to their ability to potentiate immune responses. In this study, we evaluated the immunogenicity and protective efficacy of heteromorphous mesoporous silicon microparticles (MSMPs) as an adjuvant in the context of SARS-CoV-2 vaccination. MSMPs conjugated with the S1 subunit of the spike protein (MSMPs-S1) elicited a robust and sustained humoral immune response in BALB/c mice, comparable to that induced by aluminum-based adjuvants. Following a booster dose, MSMPs-S1 significantly increased IgG2a titers and neutralizing antibody levels, surpassing those observed with $Al(OH)_3$-based formulations. In addition, MSMPs-S1 enhanced cellular immunity, as reflected by higher IFN-γ production in T cells relative to the

ARTICLE IN PRESS

aluminum-adjuvanted group. In k18-hACE2 transgenic mice, vaccination with MSMPs-S1 conferred protection against a lethal SARS-CoV-2 challenge, resulting in marked reductions in viral loads in both lung and brain tissues. In vitro, stimulation of human peripheral blood mononuclear cells (PBMCs) with MSMPs-S1 increased IFN-γ production in T cells, particularly in the presence of dendritic cells. Collectively, these findings support the potential of MSMPs as an effective adjuvant capable of promoting both humoral and cellular immunity, with relevance for the development of vaccines targeting emerging viral pathogens.

KEYWORDS

Vaccine, Virus, Cytotoxic, Mesoporous Silicon Microparticles

Introduction:

The use of adjuvants in vaccine development is critical for eliciting strong and sustained immune responses, particularly given the limited immunogenicity of subunit antigens compared with whole pathogens [1]. Consequently, the identification of new adjuvants that are both safe and effective has become a central objective in vaccine research. Since 1925, only a limited number of adjuvant classes have been approved for human use, most notably aluminum hydroxide, each presenting specific drawbacks that restrict their broader applicability [2].

The encapsulation of recombinant proteins in inorganic micro- and nanoparticles is an emerging strategy, as these particles can activate antigen-presenting cells and other immune cells while also being efficiently phagocytosed [3,4]. Mesoporous silica microparticles (MSMPs), fabricated by the electrochemical etching of silicon wafers, offer several advantages over mesoporous silica nanoparticles (MSNs) produced by other methods. Their pores can be engineered to be larger (ranging from 2 to more than 250 nm), and they form heterogeneous populations of nano- and microparticles that are biodegradable in physiological environments. These properties make MSMPs low-toxicity carriers with high antigen-loading capacity and controlled release. Their unique physicochemical characteristics allow versatile chemical derivatization, while their ease of production, low cost, and scalability make them promising innovative adjuvants with advantages over current options.

In previous studies [5], we demonstrated for the first time that bare MSMPs containing silanol groups facilitate the loading of virus-specific class I-restricted T-cell epitopes (CEFpp) onto human monocyte-derived dendritic cells (MoDCs), and that enhanced viral peptide presentation correlates with a more efficient generation of antiviral cytotoxic T lymphocyte (CTL) responses. This process, known as cross-presentation, is essential for activating adaptive immunity against viral and tumor antigens in vaccine development.

ARTICLE IN PRESS

During the SARS-CoV-2 pandemic, vaccines played a crucial role in preventing severe illness and death [6]. However, as observed with other coronaviruses in different species, vaccine-induced protection wanes over time. Epidemiological studies have shown that antibody levels decline after six months, increasing susceptibility to reinfection and severe disease [7,8]. Moreover, T-cell responses play a key role in resolving viral infection and, in the long term, in establishing durable immune memory. Virus-specific memory $CD8^+$ T cells can persist for up to six years after SARS-CoV infection, even when memory B cells and virus-specific antibodies are no longer detectable [9].

Experience with other pathogenic coronaviruses, such as SARS-CoV and MERS-CoV, has shown that effective protection requires vaccines to elicit not only strong antibody responses but also robust cellular immunity, including virus-specific $CD4^+$ and $CD8^+$ memory T cells [10]. For example, memory $CD8^+$ T cells targeting an immunodominant epitope protected aged mice from fatal SARS-CoV infection through cytolytic mechanisms and the production of cytokines such as IFN-γ, TNF-α, and IL-2, dramatically reducing viral loads in the lungs [11].

In this work, we provide new evidence demonstrating the ability of MSMPs to induce a specific, protective, and long-lasting immune response characterized by potent cellular and humoral immunity with high neutralizing capacity against experimental SARS-CoV-2 infection. Furthermore, we show that MSMPs enhance the stimulation of human peripheral blood mononuclear cells (PBMCs) from immunized individuals in response to SARS-CoV-2 S1 protein peptides.

ARTICLE IN PRESS

Results

1.-MSMPs-Spike induce a robust SARS-CoV-2-specific immune response

1.1 MSMPs promote long-lived humoral responses with neutralizing antibodies

To evaluate humoral responses and neutralizing antibody production, mice were immunized on days 1, 30, and 203 after the first dose, with the final administration serving as a booster. Sera were collected on days 0, 30, 60, 150, and 210, the latter corresponding to the study endpoint.

The levels of total IgG and IgG1 antibodies against the SARS-CoV-2 S1 protein measured in the serum of immunized animals at days 30, 60, and 210 remained comparable between the silicon-based and aluminum-based vaccine formulations (Figure 1). However, following the booster dose on day 203, IgG2a levels were significantly higher in the silicon-based vaccine complex compared with the aluminum-based formulation, although both vaccine complexes induced increases in total IgG and IgG1. These results demonstrate that MSMPs elicit a strong humoral

ARTICLE IN PRESS

response comparable to that induced by $Al(OH)_3$ and superior to that generated by the antigen alone. Notably, for IgG2a, the humoral response after the booster dose was stronger than that induced by $Al(OH)_3$.

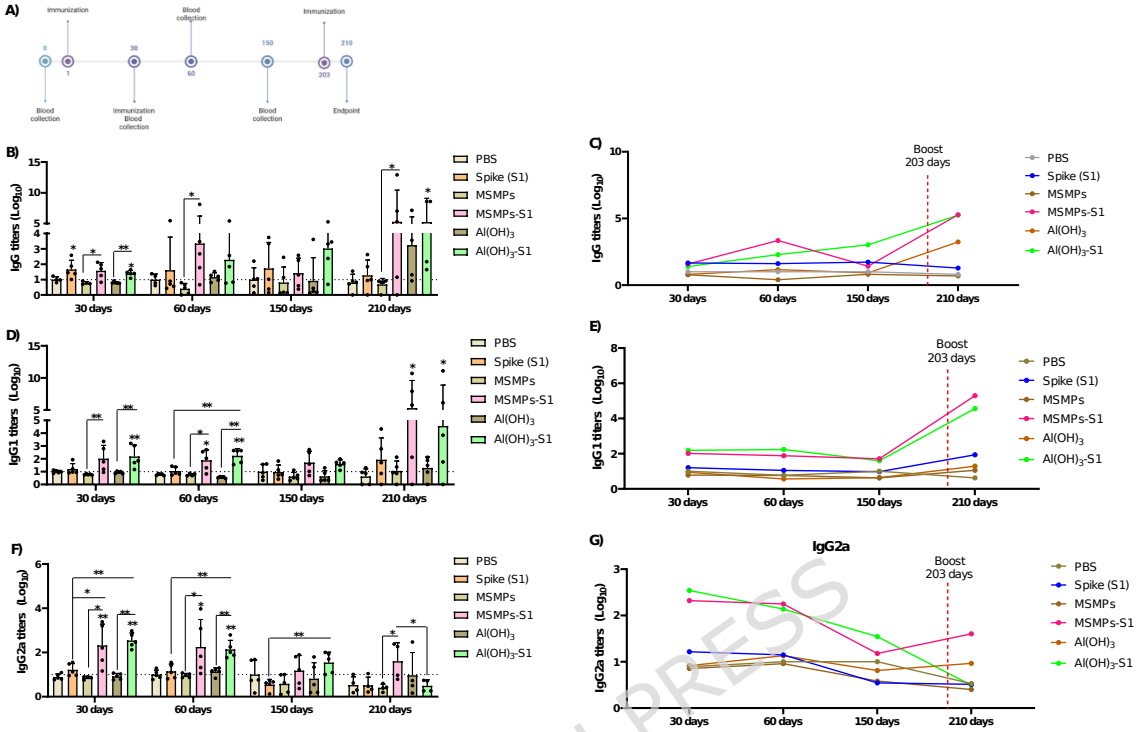

Figure 1: Humoral response in BALB/c mice immunized against SARS-CoV-2. A) Schematic representation of the immunization protocol followed in the study. Panels B, D, F show individual Igs values (log_{10}) with variability; panels C, E, G show group means to highlight kinetics. **B-C)** Total IgG, **D-E)** IgG1 and **F-G)** IgG2a antibody production against the S1 subunit in BALB/c mice immunized with Spike, MSMPs-S1 and $Al(OH)_3$-S1 over six months following three doses of the vaccine complex. Serum was collected on day 0, 30, 60, 150 and 210 after the first dose. Serum samples were diluted in PBS 1/400 to analyze IgG and IgG1 and 1/200 to analyze IgG2a, and results were normalized to PBS controls obtained at each time point. Statistical significance was determined using the Mann-Whitney U test. *p< 0.05, **p < 0.01, ***p < 0.001. n=5.

Since we demonstrated that MSMPs induced the production of Spike-specific IgG, IgG1, and IgG2a antibodies, we next evaluated their ACE2–RBD neutralizing capacity using a competitive ELISA assay. Neutralization levels were comparable among groups immunized with $Al(OH)_3$ and silicon at days 30, 60, and 150. However, following the booster dose on day 210, only the MSMPs–S1 complexes elicited a significant increase in neutralizing activity, which positively correlated with IgG, IgG1, and IgG2alevels (Figure 2A and 2B).

ARTICLE IN PRESS

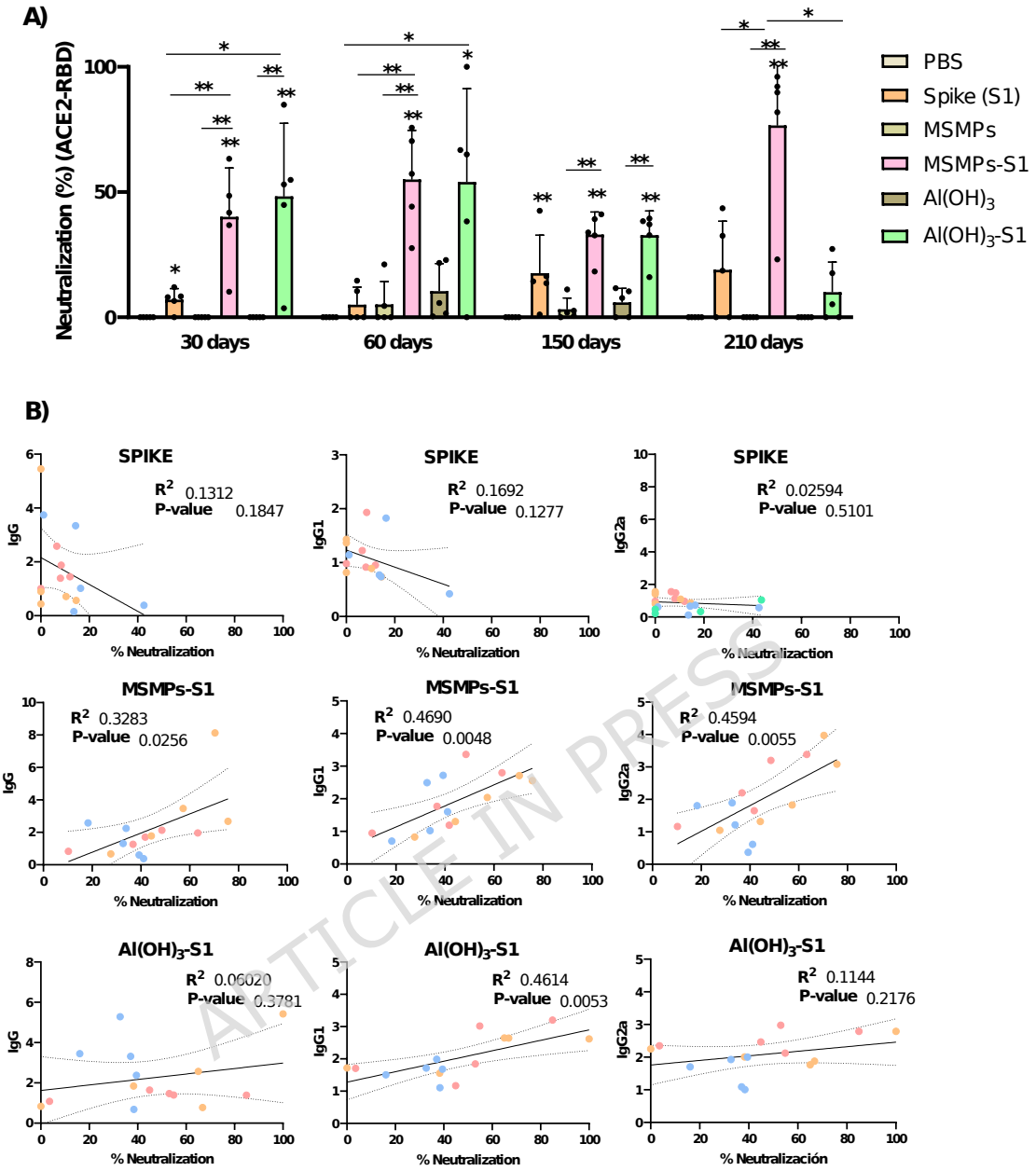

Figure 2: Neutralization response in BALB/c mice immunized against SARS-CoV-2. A) Percentage of neutralization in BALB/c mice immunized with S1 in combination with MSMPs or $Al(OH)_3$ **B)** Correlation between total IgG, IgG1 and IgG2a antibody titers and and the percentage of neutralizationin BALB/c mice immunized with Spike, MSMPs-S1 or $Al(OH)_3$-S1 at 30 (pink), 60 (orange), and 150 (blue) days after the first immunization. Results were normalized to PBS controls obtained on day 30.

In this study, we implemented a vaccination protocol similar to those used in human populations, utilizing the wild-type (WT, Wuhan variant) SARS-CoV-2 Spike antigen. We then examined how mutations in various SARS-CoV-2 variants (Delta, Beta, and

ARTICLE IN PRESS

Omicron) affected the Spike-specific antibodies generated after WT-Spike immunization, as well as the neutralizing activity of these sera in mice, assessed through RBD-binding inhibition. Our findings showed that although mice developed Spike-specific and neutralizing antibodies against the wild-type RBD, they failed to generate neutralizing antibodies against the Omicron variant. No significant differences were observed for the Delta or Beta variants compared with the response to the original virus (Figure 3).

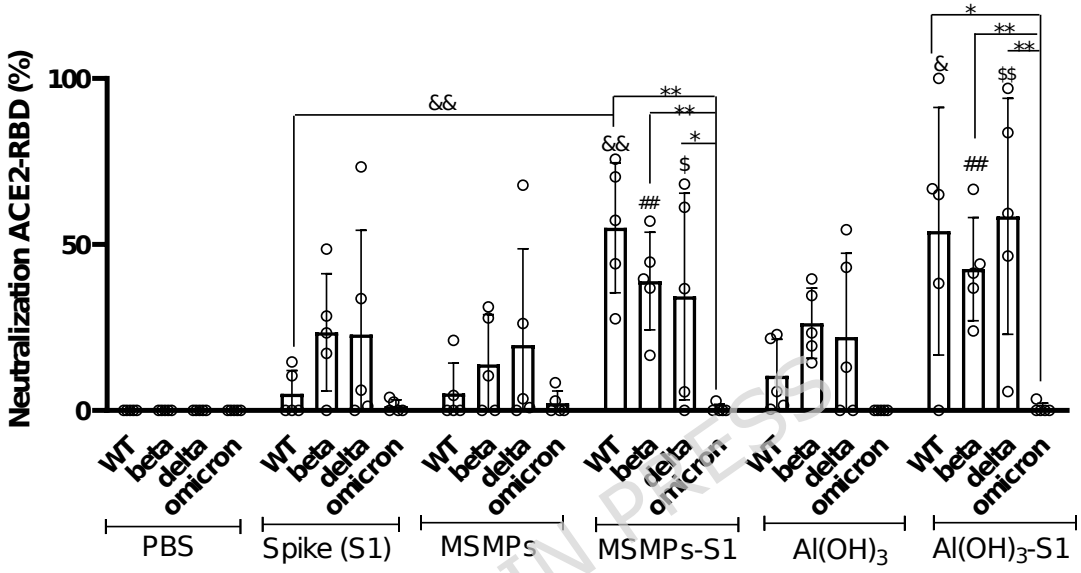

Figure 3: Neutralization activity against SARS-CoV-2 variants in BALB/c mice Percentage of neutralization against different SARS-CoV-2 variants of concern (VOCs) in BALB/c mice immunized with Spike, MSMPs-S1 and $Al(OH)_3$-S1 measured 30 days after the first dose. Results were normalized to PBS controls obtained at day 30. Statistical analysis was performed using the non-parametric Mann–Whitney test. Symbols indicate significant differences: **&** for comparisons with the Wild- type variant, **#** for the β variant, **$** for the Δ variant and * for comparisons between between variants within the same group. Significance levels are indicated by the number of symbols (one, $P < 0.05$; two, $P < 0.01$; three, $P < 0.001$). n=5.

1.2 MSMPs-S1 vaccine complex improves the specific $CD3^+CD4^-$ T-cell response

Considering the importance of T cells during the immune response to SARS-CoV-2, we sought to determine whether T lymphocytes from MSMPs-Spike vaccinated mice responded differently to Spike-specific peptides compared with unvaccinated mice and those immunized with $Al(OH)_3$-S1. Our results showed that the MSMP-Spike

ARTICLE IN PRESS

complex induces a strong cellular response, as measured by IFN-γ production from $CD3^+CD4^-$ T cells isolated from the spleens of mice immunized with this complex and restimulated *in vitro* with S1. This response was higher than that observed in splenocytes from animals immunized with $Al(OH)_3$-Spike, comparable between both vaccine complexes under PMA/Ionomycin stimulation (supplementary Figure 2), and significantly higher than that induced by Spike alone (Figure 4).

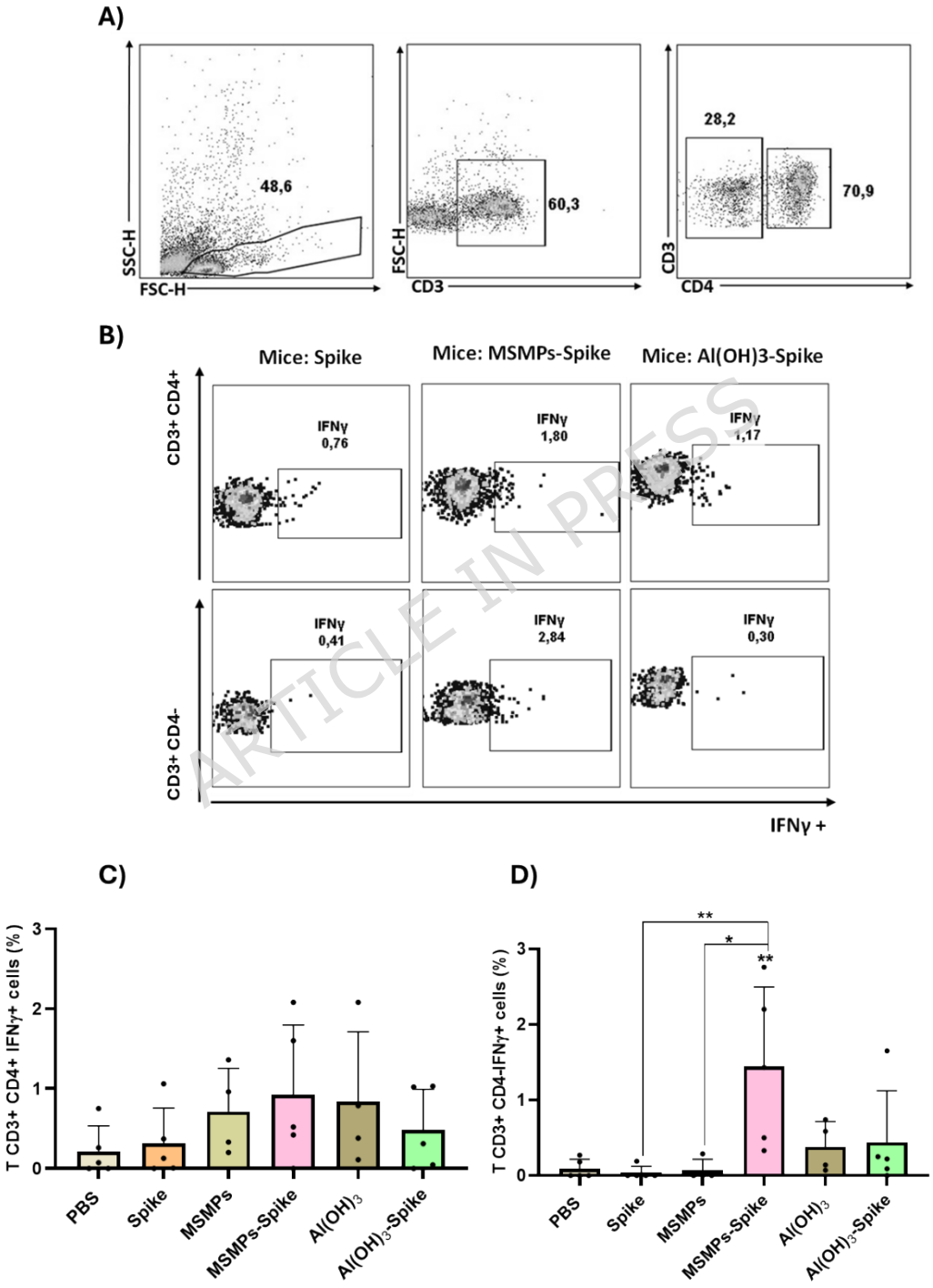

Figure 4: *In vitro* cellular response in BALB/c mice immunized against SARS-CoV-2. A) Gating strategy used to analyze IFN-γ production in $CD4^+$ and $CD4^-$ T

ARTICLE IN PRESS

lymphocytes **B)** Representative dot plots showing IFN-γ production in $CD3^+CD4^+$ and $CD3^+$ $CD4^-$ T cells from BALB/c mice immunized with S1, MSMPs-S1 and $Al(OH)_3$-S1. **C)** Th2 cellular response from $CD4^+$ T cells in different groups. **D)** Th1 cellular response from $CD3^+CD4^-$ T cells in different groups. Results represent the mean percentages (%)normalized after subtraction of basal stimulation. Immunization groups: Spike (orange), MSMPs-S1 (pink) and $Al(OH)_3$-S1 (green). Statistical significance was determined using the Mann-Whitney U test. *p < 0.05, **p < 0.01, ***p < 0.001. n=4**.**

2.- MSMPs-Spike vaccination induces protection in K18-hACE2 mice

Following a two-dose immunization schedule over one month (Figure 5A), IgG1 levels measured one week after the final immunization were comparable between MSMPs-S1 and $Al(OH)_3$-S1 groups and significantly higher than those induced by Spike alone (Figure 5B), consistent with our previous findings. One week after the last immunization, all mice were infected via intranasal route. Mice injected with PBS, MSMP, or S1 alone died between days 5 and 8 post-infection. In contrast, only one mouse immunized with MSMPs-S1 and none immunized with $Al(OH)_3$-S1 succumbed to infection (Figure 5C). All infected mice treated with PBS, MSMP or S1 exhibited progressive weight loss until death (Figure 5D).

To further assess disease progression, additional clinical parameters were monitored daily (Supplementary Figure 3A, B). No significant differences were observed between mice immunized with MSMPs-S1 and those immunized with $Al(OH)_3$-S1.

ARTICLE IN PRESS

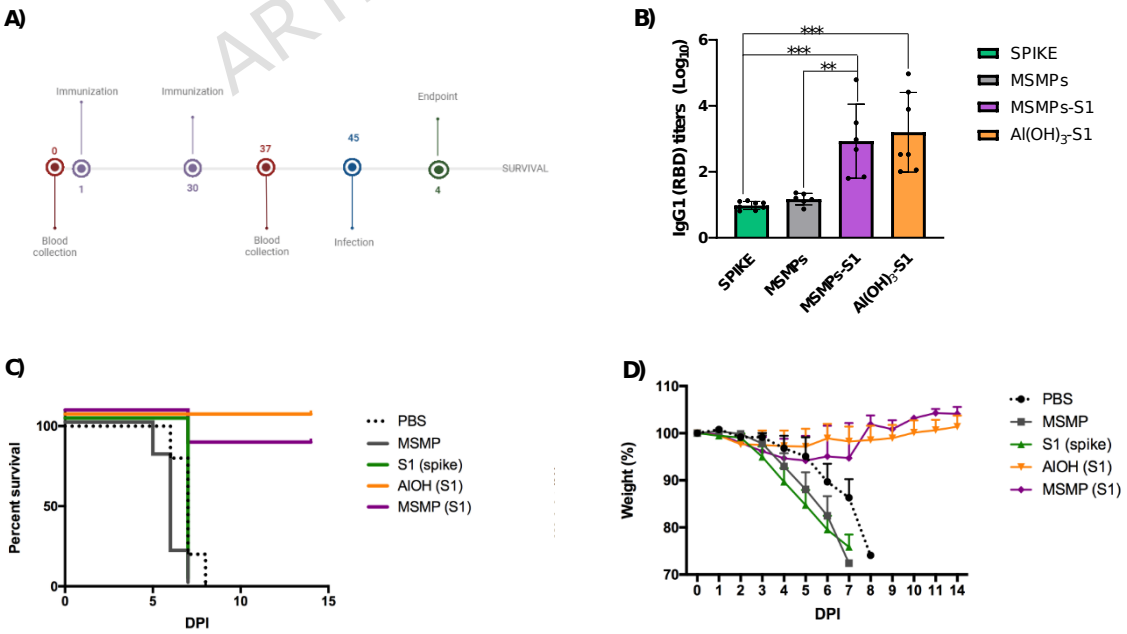

Figure 5: SARS-CoV-2 infectivity assay in K18 $hACE_2$ mice. A) Schematic representation of the immunization and infectivity protocol used in the study. **B)**

ARTICLE IN PRESS

IgG1 antibody production against the RBD 37 days after the first immunization. Data were normalized to PBS control, and statistical significance was determined using the Mann-Whitney test. *p < 0.05, **p < 0.01, ***p < 0.001. **C)** Survival curve of immunized mice. **D)** Daily weight variations over 15 days after infection (Mean ± SEM). Control groups included PBS (dotted line) and MSMPs (gray), while antigen-immunized groups included S1 (green), MSMPs-S1 (purple) and $Al(OH)_3$-S1 (orange). n=5.

The presence of viral RNA in different organs was also evaluated. In the lungs the primary target organ of this virus, animals immunized with MSMPs-S1 or $Al(OH)_3$S1 showed lower viral levels compared with PBS- treated controls or mice immunized with the S1 antigen alone. No Viral RNA was detected in the heart of any animal. In the brain, an organ for which the virus has a strong tropism, animals immunized with $Al(OH)_3$-S1 or MSMPs-S1 displayed significantly reduced viral levels compared with the PBS control group or mice immunized with S1 alone. (Figure 6)

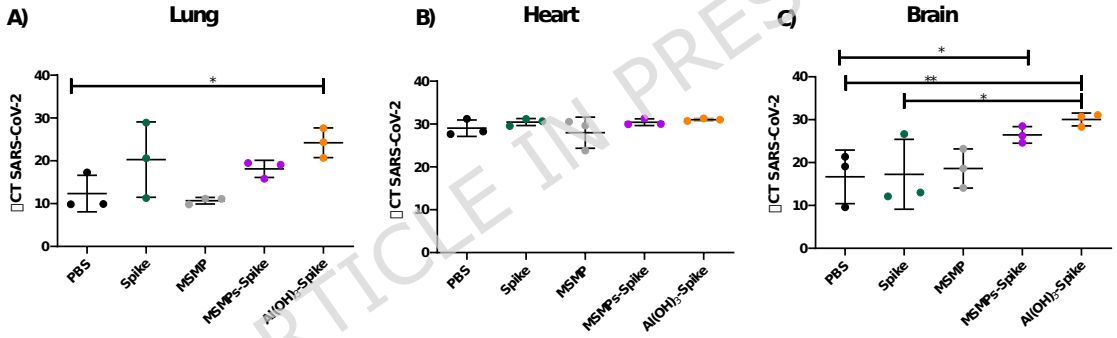

Figure 6: Viral load after infection in k18 hACE2 mice. SARS-CoV-2 viral load detected four days after infection in the **A)** lung **B)** heart and **C)** brain of K18 hACE2 mice immunized with PBS (black), Spike (green), MSMPs (gray), MSMPs-S1 (purple) and $Al(OH)_3$-S1 (orange). Statistical significance was assessed using one-way ANOVA *p < 0.05, **p < 0.01, ***p < 0.001.

3.- MSMPs-Spike enhances *in vitro* IFN-γ production in human lymphocytes

To investigate the effect of MSMPs in humans, we performed *in vitro* experiments using peripheral blood mononuclear cells (PBMCs) from donors who had been exposed to the SARS-CoV-2 during the pandemic, either through infection or vaccination (as confirmed by the presence of virus-specific antibodies; Supplementary Figure 4). In vaccinated donors, we observed a significant increase in IFN-γ production. Specifically, the proportion of $CD3^+$cells that responded *in vitro* to viral peptides (Peptivator S) by producing IFN-γ was significantly higher when these peptides had been pre-incubated with MSMPs (Figure 7).

ARTICLE IN PRESS

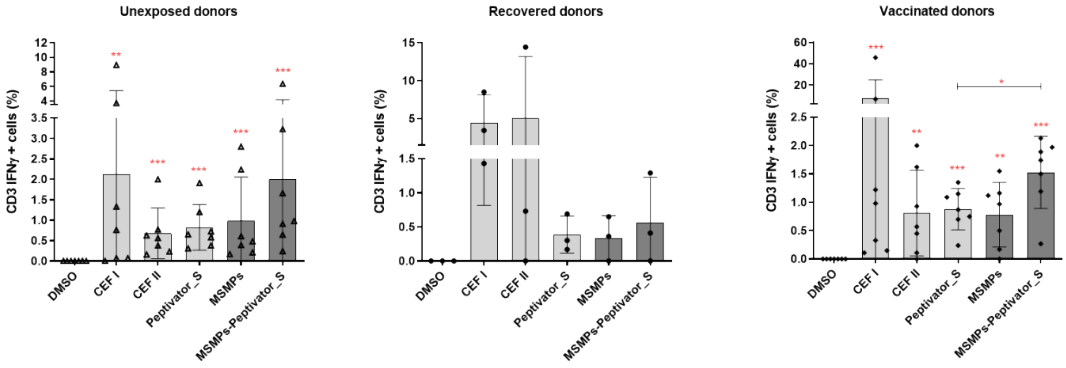

Figure 7: *In vitro* IFN-γ production in T cells. Significant increase in IFN-γ production in response to MSMPs conjugated with SARS-CoV-2 peptides after one week of stimulation with Spike peptides. IFN-γ levels were measured on days 0 and 6. Statistical significance was determined using the Mann-Whitney test. *$p < 0.05$, **$p < 0.01$, ***$p < 0.001$.

Moreover, we analyzed IFN-γ production by $CD3^+CD4^+$ and $CD3^+CD4^-$ cells after seven days of PBMCs culturing with different stimuli (Figure 8), following the same approach used for $CD3^+$ cells. We then compared these results with those obtained after co-culturing the PBMCs with autologous Monocyte derived Dendritic Cells (MoDCs), that had been pretreated with the same stimuli. Our observations showed that when peptivator S was pre-loaded onto MSMPs, the specific IFN-γ production by $CD3^+CD4^-$ T lymphocytes significantly increased compared with MSMPs–Peptivator S samples that had not been pre-treated. No changes were observed in $CD4^+$ cells. When MSMPs-S1 or Peptivator S were first exposed to MoDCs, a general increase in IFN-γ production was detected, although no differences were observed between treatment groups (Figure 8).

ARTICLE IN PRESS

ARTICLE IN PRESS

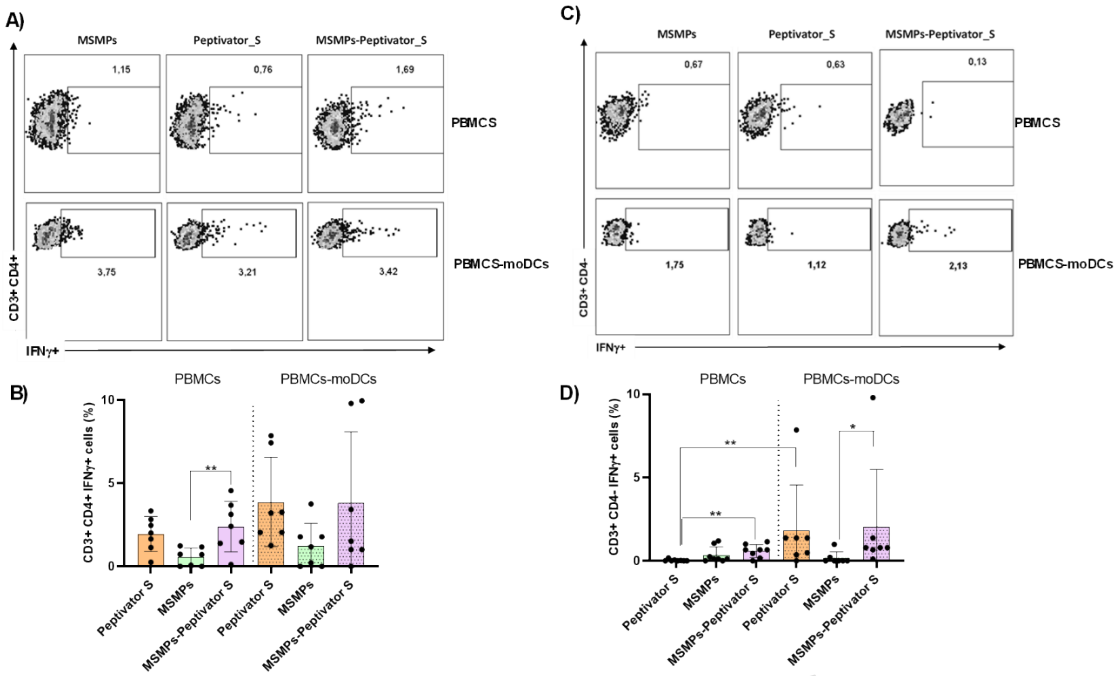

Figure 8: ***In vitro*** **IFN-γ production in T cells.** **A)** Representative dot plots showing IFN-γ production in $CD4^+$ T cells after co-culture of PBMCs with previously stimulated moDCs and without co-culture. **B)** $CD3^+$ $CD4^+$ T response (IFN-γ production) in the presence and absence of moDCs. Results represent the mean percentage obtained, normalized after subtraction of basal stimulation. **C)** Representative dot plots showing IFN-γ production in $CD3^+CD4^-$ T cells after co-culture of PBMCs with previously stimulated moDCs and without co-culture. **D)** $CD3^+CD4^-$ T response (IFN-γ production) in the presence and absence of moDCs. Results represent the mean percentage obtained (normalized after subtraction of basal stimulation). Statistical significance was determined using the Mann-Whitney test. *P < 0.05, **P < 0.01, ***P < 0.001. n=7

ARTICLE IN PRESS

Discussion:

One of the most critical strategies for developing effective vaccines is the selection and use of appropriate adjuvants, which are essential to enhancing vaccines potency by eliciting a robust immune response. The formulation of new vaccines incorporating potent and safe adjuvants is necessary to achieve protective and long-lasting immunity. Silica-based materials have emerged as promising candidates both

ARTICLE IN PRESS

as delivery vehicles and adjuvants. Navarro-Tobal et al. demonstrated that mesoporous silica particles were able to induce a prolonged humoral response in a peptide-based vaccine, lasting up to 52 days after immunization [14].

Silicon particles of various sizes and shapes have been engineered, including mesoporous silica nanoparticles (MSNs) and mesoporous silica microparticles (MSMPs). In both formats, their capacity to transport proteins-either within their pores or chemically bound to their surface-has been well established. Currently, mesoporous silica nanoparticles are being evaluated in mouse immunization studies to assess their adjuvant potential against different diseases. In both nanoparticles and microparticles, pore size can be tuned, allowing the loading of molecules of different dimensions, with the size of the molecule, the pore diameter, and the release rate being directly related [15]. Silicon-based particles have demonstrated immunostimulatory properties; however, important differences arise depending on their size, shape and surface functionalization, all of which may play a key role in modulating the immune response [15–19]. The results presented in this manuscript confirm that heterogeneous Mesoporous Silicon Microparticles (MSMPs) function as a effective adjuvant. Our vaccine complex based on amino-modified (MSMPs-S1) was capable of activating both humoral and cellular immune responses against SARS-CoV2 after two doses. On the one hand, it stimulated a durable and neutralizing virus-specific humoral response that was superior to that observed in mice immunized solely with spike protein and comparable to the response elicited by the aluminium-based formulation. The neutralizing capacity of this response declines after five months in both the MSMP- and aluminum-based vaccines, a pattern similar to that described for other SARS-CoV2 vaccines in humans [20,21].

Interestingly, significant differences emerge when a booster dose was administered after 203 days. In this case, only the MSMPs-S1 complex was capable of inducing a strong neutralizing humoral response, surpassing the neutralization observed in sera collected at one, two or five months. In humans, Flaxman A. et al. reported that immunogenicity following a delayed second dose or a third dose of ChAdOx1 nCoV-19 is influenced by the interval between doses, with longer intervals leading to enhanced antibody responses and greater vaccine effectiveness [23]. Notably, in our experiment, the levels of Spike-specific total IgG and IgG1 after the booster were comparable between animals immunized with MSMPs and those receiving the $Al(OH)_3$ adjuvant. However, only the animals immunized with silica generated significant levels of Spike-specific IgG2a. This difference may reflect the distinct immune profiles elicited by each adjuvant: MSMPs might primarily enhance a Th1-like response, which is associated with IgG2a production and may enhance cytotoxic T-cell activation and memory formation, whereas $Al(OH)_3$ promotes a Th2-skewed response, favoring IgG1 production [24].

ARTICLE IN PRESS

Long lasting humoral responses have been described in immunization experiments using silica particles. Navarro-Tovar et al. reported that mesoporous silicon microparticles can induce humoral responses in peptide-based vaccination, maintaining antibody levels up to 52 days in a four-immunization protocol [14]. In this study we demonstrate that MSMPs-Spike immunization elicits antibody responses lasting over 210 days with only three immunizations using amino-functionalized silica particles. Differences in size distribution (3 ± 1 µm for Porous Silicon Particles (PSiP) vs 0.5 µm forMSMPs) and surface charge (oxidized PSiP vs amino-modified MSMPs) may account for these discrepancies.

Regarding SARS-CoV-2 immunization, Adam et al., observed that BALB/c mice immunized with modified silicon microparticles loaded with the TLR9 ligand cytosine guanosine dinucleotide (CpG), and the STING agonist 2´-3´ cyclic GAMP (cGAMP), conjugated to the RBD region (mSMP-RBD), developed high titers of IgG1, IgG2a and IgG2b, comparable to those induced by alum-RBD [25]. Moreover, antibody levels were sustained for up to 180 days after immunization. Differences in the immunogen (S1 vs. RBD), dosage (4.5 µg vs. 5-25 µg), microparticles size (3.5 µm vs 0.5 µm), and immunization protocols may explain the variations observed between their results and ours.

MSMPs-Spike immunization not only induces a strong and long-lasting IgG anti-Spike antibody response but also enhances the ACE2-RBD neutralizing activity of these antibodies nearly abolishing ACE2 binding to RBD protein, whereas $Al(OH)_3$ fails to elicit this response. This neutralizing activity has been shown to prevent viral entry and, consequently, infection [26]. Our results show that the *in vitro* neutralizing capacity of sera obtained at 30, 60, and 150 days is comparable between animals immunized with silicon-based and aluminum-based formulations, consistent with the similar levels of S1-specific immunoglobulins detected in these samples. Interestingly, the highest neutralizing capacity is observed after the booster dose in mice immunized with MSMPs-S1, in contrast to the practically absent neutralizing capacity in sera from mice immunized with $Al(OH)_3$-S1. This correlates with the very low Spike-specific IgG2a levels detected in the aluminum-immunized group. It is also possible that the immunoglobulins from mice immunized with MSMPs-S1 after the boost have a higher affinity and therefore greater neutralizing capacity than those from $Al(OH)_3$-S1–immunized mice. Importantly, the neutralization levels achieved after only two immunizations were sufficient to effectively protect mice from experimental infection with a lethal dose (10^5 PFU) of the virus in both aluminum-based and silicon-based vaccines. Intramuscular MSMPs-S1 immunized mice also showed a significant reduction in viral load in the brain-comparable to that observed in $Al(OH)_3$-S1–immunized mice—following lethal challenge. This is a crucial finding, as the strong tropism of the virus for the brain is typically the primary cause of

ARTICLE IN PRESS

mortality in mice [27]. Furthermore, preliminary lung histology at day 7 post-infectionrevealed scattered inflammation but clear signs of alveolar parenchyma recovery in MSMPs-S1–vaccinated mice, comparable to those immunized with $Al(OH)_3$-S1.

SARS-CoV-2 variants carry mutations in the RBD of the Spike protein that may affect antibody binding following WT-Spike immunization [27,28]. Our antibody neutralization studies revealed that the neutralizing capacity of sera from WT-Spike-immunized animals against different SARS-CoV-2 variants (Wuhan, Beta, Delta, and Omicron) was comparable between silicon- and aluminum-based vaccine complexes. The B.1.35 (Beta) and B1.617 (Delta) variants exhibited a neutralization percentage similar to the wild-type strain, as both contain a limited number of RBD mutations that do not impair the binding of neutralizing antibodies. In contrast, the absence of neutralization against the B.1.1529 (Omicron) variant is consistent with its high number of RBD mutations.

T cells, particularly cytotoxic $CD8^+$ T lymphocytes, play a central role in eliminating virus infected cells, including those targeted by SARS-CoV-2 and other infectious agents [5, 30]. Studies on other SARS-CoV viruses have shown that $CD8^+$ memory T cells can persist for up to six years post-infection, whereas memory B cells were not detected over such an extended period [9]. Moreover, in aged mice, antigen-specific $CD8^+$ T cells have been shown to protect against fatal SARS-CoV infection through the release of cytokines such as IFN-□ and TNF-α, which contribute to reducing viral load in the lungs [11]. In this context, our results demonstrate that MSMPs-S1 immunization induces a robust cellular response, as evidenced by-antigen specific IFN-γ-producing $CD3^+CD4^-$ T-cells- most of which are $CD8^+$-that persists for at least seven months after the initial immunization. This long-lasting response was not observed in mice immunized with the aluminum-based vaccine. One possible explanation is that $Al(OH)_3$ primarily stimulates macrophages but is less effective at activating dendritic cells and Toll-like receptors, which are essential for strong T-cell priming [31].

In humans, our results show that MSMPs enhance the "*in vitro*" INF-γ response of SARS-CoV-2 peptide specific T-cells from healthy donors, particularly in the presence of dendritic cells as antigen-presenting cells. In these experiments, the responding T lymphocytes consist of memory cells previously activated *in vivo* in the donor individuals. These findings are consistent with our earlier observations showing that MSMPs, efficiently induce the maturation of Monocyte Derived Dendritic Cell (MoDCs) and enhance CEF (cytomegalovirus, Epstein-Barr virus, and influenza virus) peptide-specific memory T-cell stimulation *in vitro* [5].

ARTICLE IN PRESS

Together, these results support the role of MSMPs as potent activators of T lymphocyte-mediated immunity. Although aluminum salts have been the most widely used adjuvants for more than seven decades, they present well-recognized limitations, including poor induction of Th1-type responses. These limitations underscore the need for new adjuvants capable of eliciting more balanced and effective cellular immunity [2,31]. In conclusion, this work demonstrates that MSMPs enhance a long-lasting cellular and humoral protective responses against SARS-CoV-2 in mice. Additionally, these particles improve memory T-cell responses in humans, highlighting their potential as a promising next-generation vaccine adjuvant.

Methods:

Donors:

Peripheral blood mononuclear cells (PBMCs) were isolated from blood obtained from healthy adult donors in 2021. Although exact dates of infection or vaccination were not available for all recovered individuals, all samples were collected more than one month after documented SARS-CoV-2 infection or vaccination and within six months of that event. Donors had either been infected with SARS-CoV-2 or vaccinated with different vaccine regimens during the study period. Ethical approval was obtained from the appropriate ethics committee, and all participants written informed consent.

Mice:

Thirty female BalB/c mice (8 weeks old) were obtained from Charles River company (USA) and housed in a specific pathogen-free facility at the Complutense University of Madrid (UCM).

Additionally, forty K18-hACE2 transgenic mice were used to evaluate the protective effects of mesoporous silicon microparticles (MSMPs) against SARS-CoV-2 infection. These mice were housed under sterile conditions in ventilated racks at the Centro de Investigación en Sanidad Animal (CISA), where infections and euthanasia procedures were performed under Biosafety Level 3 conditions.

Mice were anesthetized with isoflurane administered via inhalation using a precision vaporizer connected to an induction chamber. Isoflurane concentrations for anesthesia induction ranged from 3% to 5% in oxygen, while maintenance was achieved at 1.5% to 2.5%. At the end of the study, mice were euthanized using a two-step method: deep anesthesia was first induced with isoflurane via inhalation to ensure loss of consciousness and minimize pain or distress, followed by cervical dislocation as the physical method of euthanasia to ensure death.

ARTICLE IN PRESS

Ethic declaration:

The animal study was reviewed and approved by the Ethics Committees of the Consejo Superior de Investigaciones Científicas (CSIC), the Universidad Complutense de Madrid, and the Comunidad Autónoma de Madrid (approval reference: PROEX 272.5/22). All experimental procedures were conducted in accordance with relevant institutional and national guidelines and regulations. Furthermore, all methods are reported in accordance with the ARRIVE guidelines (https://arriveguidelines.org) for the reporting of animal research. The studies involving human participants were viewed and approved by Ethics Committee of Hospital Clínico San Carlos (21/200-E). All participants provided written informed consent prior to inclusion in the study, and research was performed in accordance with the Declaration of Helsinki. Samples were anonymized prior to analysis to ensure confidentiality and data protection.

MSMPs production and functionalization

Mesoporous silicon microparticles (MSMPs) were produced and characterized following previously described methodologies [5,12]. Briefly, silicon wafers were electrochemically treated with hydrofluoric acid (48% HF) and ethanol (96% EtOH) in a 1:1 ratio. The resulting mesoporous layerswere collected, manually milled, and sieved to obtain particles ≤5 µm, as optimized in earlier experiments [5]. These particles were then functionalized with amino groups using (3-Aminopropyl) triethoxysilane (APTS) (Sigma-Aldrich, St. Louis, MO, USA). The characterization of MSMPs is shown in Supplementary Figure 1.

Antigen loading

Peptide pools derived from SARS-CoV-2 (PepTivator® S, Miltenyi Biotec, Germany), consisting of 15-mer peptides overlapping by 11 amino acids and covering immunodominant regions of the spike glycoprotein, were loaded onto MSMPs-NH_3 following previously described protocols [5,12]. To assess MSMP loading capacity, peptide-loaded MSMPs were centrifuged (10 min, 10,000 × g, 4 °C). The supernatant was discarded, and the pp-MSMP pellet was resuspended in 50 µL of PBS and incubated for 24 hours at room temperature. After a second centrifugation (10 min, 10,000 × g, 4 °C), the peptide concentration in the supernatant was measured using a NanoDrop spectrophotometer at 280 nm. The peptide concentration consistently ranged between 40 and 60 µg/mL (2–3 µg total), indicating that at least 20–30% of the peptides in the original solution were successfully loaded into the MSMPs. Considering that 1 µg/mL of peptides corresponds approximately to a 1 µM concentration, it can be estimated thateach particle is capable of loading a minimum of 1.2×10^7 viral peptides.

ARTICLE IN PRESS

PepTivator®peptide pools bound to MSMPs were used to stimulate human PBMCs *in vitro*, whereas S1 protein bound to MSMPs was used for mice immunization. Each mouse received 4.5 µg of SARS-CoV-2 Spike S1 protein either alone or formulated with adjuvants: aluminium hydroxide ($Al(OH)_3$) or MSMPs (0.64 mg/mouse). CEF I and CEF II peptide pools (Mabtech, Swiden) were used as standardized peptide pools to evaluate $CD3^+CD4^-$ T and $CD3^+CD4^+$ T cell responses in human PBMCs.

Immunization protocol:

The gene encoding the SARS-CoV-2 Spike S1 protein was cloned into the commercial pCAGGS vector, propagated in *E. coli* DH5α, and purified using the Gigaprep Kit (Qiagen). Transient protein expression was carried out using the Expi293F Expression System (Thermo Fisher Scientific). Cells were cultured in suspension at 37°C in a humidified incubator (≥80% humidity, 8% CO_2) with agitation. Cultures were passaged at least three times to ensure optimal doubling time and viability (>90%). Transfections were carried out at a final culture volume of 150 mL, and cultures were incubated post-transfection for seven days under the same conditions. For purification, the supernatant was collected and clarified by centrifugation (17000×g, 45 min, 4°C). The supernatant was incubated with Ni-NTA resin (Invitrogen) for 2 h at 4°C with gentle rocking. The resin was packed into a gravity-flow column and washed sequentially with PBS and PBS 25 mM imidazole. Bound protein was eluted with PBS containing 250 mM imidazole. Eluted fractions were analyzed by SDS-PAGE, pooled, dialyzed against PBS to remove imidazole, concentrated using centrifugal filter units (Centricon, 10kDa MWCO) and quantified by absorbance. Aliquots of 50 µg were flash-frozen in liquid nitrogen and stored at –80°C until use.

ARTICLE IN PRESS

BalB/c mice were immunized three times (days 1, 30 and 203) intramuscularly (IM). Sera were collected on days 0, 30, 60, 150 and 210. In virus-challenge experiments, k18-hACE2 transgenic mice were immunized twice via IM injection with a four-week interval between doses (days 1 and 30). Sera were collected at days 0 and 37. Each mouse received 4.5 µg of SARS-CoV-2 Spike S1 protein either alone or formulated with adjuvants: aluminum hydroxide ($[Al(OH)_3]$ used as Alhydrogel® 2% (Croda Ibérica SAU; Barcelona, Spain) or MSMPs (0.64 mg/mouse).

For BalB/c mice, blood was collected at 15, 30, 60 and 150 days after the first dose. Serum was separated by centrifugation and stored at -80ºC. A booster dose was administered six months after the initial immunization, and mice were sacrificed seven days later for collection of blood, spleen, and inguinal lymph nodes.

In k18-hACE2 mice, blood samples were collected 30 days after the first dose, and an infectious SARS-CoV-2 challenge was performed 45 days after the initial immunization.

ARTICLE IN PRESS

Enzyme-linked immunosorbent assay (ELISA):

To quantify immunoglobulin levels, 96-well plates were coated with 5 µg/well of SARS-CoV-2 S1-His-tagged spike protein (Bionova) and incubated overnight at 4°C. Plates were washed with PBS containing 0.1% Tween-20 and blocked with 5% bovine serum albumin (BSA) in PBS for 1 h at room temperature. Serially diluted serum samples were added and incubated for 1 hour, followed by detection with HRP-conjugated secondary antibodies: anti-mouse IgG (1:1000; Invitrogen), anti-mouse IgG1 (1:2000; Invitrogen), and anti-mouse IgG2a (1:3000; Invitrogen). After 30 minutes, TMB substrate (3,3′,5,5-Tetramethylbenzidine; Sigma-Aldrich) was added, and the reaction was stopped with 1 M HCl. Absorbance was measured at 450 nm. Results were normalized to the absorbance values of PBS-immunized mice, used as negative controls.

Neutralizing antibodies assay:

A competitive ELISA was performed to evaluate the neutralization of ACE2-RBD binding. 96-well plates were coated with 2 µg/ well of SARS-CoV-2 RBD spike protein (Miltenyi Biotec) and incubated overnight at 4°C. After washing and blocking, serum samples were added and incubated for 1 h at room temperature. Biotinylated ACE2 (0.5 mg/mL; Miltenyi Biotec) was then added and incubated for 30 minutes at 37°C, followed by Streptavidin-HRP (Thermo Scientific) for 30 minutes. TMB substrate was used for color development, and reactions were stopped with 1 M HCl. Absorbance was measured at 450 nm. Neutralization percentages were calculated relative to the median absorbance of PBS-immunized control mice.

ARTICLE IN PRESS

Isolation and culture of splenocytes

Spleens from BalB/c mice were harvested and homogenized using the plunger of a sterile syringe through a 70 µm cell strainer. Red blood cells were lysed with ACK lysis buffer for 3 minutes at room temperature. Splenocytes were then seeded in 96-well plates at a density of 4×10^5 cells/ well and cultured in RPMI-1640 medium (Lonza BioWhittaker) supplemented with 10% fetal bovine serum (FBS; Gibco), 1% antibiotic–antimycotic solution (Gibco), 0.005 mM β-mercaptoethanol, and 10 U/mL murine interleukin-2 (mIL-2; ImmunoTools). To assess cellular immune responses, splenocytes were stimulated with PepTivator® S peptide pools (Miltenyi Biotec). Phorbol 12-myristate 13-acetate (PMA; 100 ng/mL) and ionomycin (1 µM) served as positive controls. Interferon-gamma (IFN-ɣ) production was evaluated by intracellular cytokine staining (ICS) and analyzed by flow cytometry.

SARS-CoV-2 Infectious challenge

Mice were intranasally inoculated with 10^5 PFU (plaque forming units) of SARS-CoV-2 viral strain Wuham Hu-1 (MAD6), kindly provided by Prof. Luis Enjuanes (CNB-

ARTICLE IN PRESS

CSIC), two weeks after the last immunization. Animals were monitored daily weighted, and scored for clinical signs as described [13]. Animals were sacrificed when they reached the humane endpoint as defined in the guidelines of the Code for Methods and Welfare Considerations in Behavioral Research with Animals EU Directive 2010/63 and Spanish regulations RD53/2013, modified by RD1386/2018).

Viral load analysis in affected organs

To evaluate viral load in target organs (lungs, brain and heart), animals (n = 5 per group) were sacrificed on days 4 and 7 post-infection (p.i.). Organs were homogenized using a 2 min cycle in a tissueLyser II (Qiagen) at maximum frequency (30Hz). Total RNA was extracted from the homogenates using the IndiSpin Pathogen extraction kit (Indical) and stored at -80ºC until analysis. Viral load was quantified by RT-qPCR using the Luna Universal Probe One-step RT-qPCR Kit (New England Biolabs) with the primers listed in Table 1.

Primers	**Sequence**
Primer N reverse	TCTGGTTACTGCCAGTTGAATCTG
Primer N forward	GACCCCAAAATCAGCGAAAT
Primer β-actina reverse	CGGACTCATCGTACTCCTGCTT
Primer β-actina forward	CAGCACAATGAAGATCAAGATCATC

Table 1: Primers used for N protein detection

ARTICLE IN PRESS

PBMCs isolation and generation of Human Monocyte Derived Dendritic Cells (MoDCs)

Peripheral blood mononuclear cells (PBMCs) were isolated from human donors by density gradient centrifugation using Ficoll-Histopaque (Cytiva). $CD14^+$ monocytes were subsequently purified by magnetic-activated cell sorting (MACS) using CD14 MicroBeads (Miltenyi Biotec), following the manufacturer's instructions. Purified monocytes were seeded into 96-well plates at a density of 0.5×10^6 cells/mL and cultured in complete RPMI-1640 medium (c-RPMI), consisting of RPMI-1640 (Lonza BioWhittaker) supplemented with 2% heat-inactivated AB human serum and 1% antibiotic–antimycotic solution (Gibco). To induce differentiation into dendritic cells, the culture medium was supplemented with 1000 U/mL recombinant human interleukin-4 (rhIL-4; ImmunoTools) and 1000 U/mL recombinant human granulocyte-macrophage colony-stimulating factor (rhGM-CSF; ImmunoTools) for 7 days.

ARTICLE IN PRESS

Co-culture of Human Monocyte Derived Dendritic cells (MoDCs) and Peripheral blood mononuclear cells (PBMCs)

PBMCs were seeded into 96-well plates at a density of 2×10^6 cells/mL in complete RPMI (c-RPMI), supplemented with 0.02 µg/mL recombinant human IL-2 (rhIL-2; ImmunoTools). Lymphocyte expansion was induced by stimulation with PepTivator® S (20 µL/mL), MSMPs (0.09 mg/mL), or MSMPs conjugated with PepTivator® S (MSMPs-PepTivator® S).

In parallel, syngeneic monocyte-derived dendritic cells (MoDCs) were stimulated with PepTivator® S (20 µL/mL), MSMPs (0.09 mg/mL), or MSMPs-PepTivator® S for 4 hours. After stimulation, PBLs were added to the MoDCs, and co-cultures were maintained in c-RPMI supplemented with 0.02 µg/mL rhIL-2 for 7 days.. Cellular immune responses were asseseed by measuring IFN-γ production in PBL and PBL–MoDC co-cultures using flow cytometry.

Intracellular cytokine Staining (ICS)

Cytokine production was assessed by ICS following a 14-hour incubation with Brefeldin A (Invitrogen). Cells were surface-stained with antibodies listed in Table 2, then fixed, permeabilized, and stained intracellulary for IFN-γ. Data were acquired on a BD FACSCelesta flow cytometer (Becton Dickinson) and analyzed with FlowJo software.

ARTICLE IN PRESS

Antibodies	Fluorophore	Clone	Target species
CD3	**APC**	**17A2**	**Mouse**
CD4	**PerCP-Cy5.5**	**GK1.5**	**Mouse**
IFN-γ	**FITC**	**XMG1.2**	**Mouse**
CD3	**APC**	**OKT3**	**Human**
CD4	**PerCP-Cy5.5**	**OKT4**	**Human**
IFN-γ	**FITC**	**4SB3**	**Human**

Table 2: Antibodies used for flow cytometry in human and mouse samples

Statistical Analysis

ARTICLE IN PRESS

Results are represented as mean ±standard deviation (SD). The Mann-Whitney U test was used for group comparisons, whereas one-way ANOVA was applied for viral load analysis in k18-hACE2 mice. Statistical significance was defined as* $p \leq 0.05$; ** $p \leq 0.01$; and *** $p \leq 0.001$.

Availability of Materials and Data:

The datasets generated and/or analysed during the current study are available from the corresponding author upon reasonable request.

References:

[1] S. K. Verma *et al.*, "New-age vaccine adjuvants, their development, and future perspective.," *Front. Immunol.*, vol. 14, p. 1043109, 2023, doi: 10.3389/fimmu.2023.1043109.

[2] B. Pulendran, P. S Arunachalam, and D. T. O'Hagan, "Emerging concepts in the science of vaccine adjuvants.," *Nat. Rev. Drug Discov.*, vol. 20, no. 6, pp. 454–475, Jun. 2021, doi: 10.1038/s41573-021-00163-y.

[3] R. Audran *et al.*, "Encapsulation of peptides in biodegradable microspheres prolongs their MHC class-I presentation by dendritic cells and macrophages in vitro.," *Vaccine*, vol. 21, no. 11–12, pp. 1250–1255, Mar. 2003, doi: 10.1016/s0264-410x(02)00521-2.

[4] R. Langer, J. L. Cleland, and J. Hanes, "New advances in microsphere-based single-dose vaccines.," *Adv. Drug Deliv. Rev.*, vol. 28, no. 1, pp. 97–119, Oct. 1997, doi: 10.1016/s0169-409x(97)00053-7.

[5] A. Jiménez-Periáñez *et al.*, "Mesoporous silicon microparticles enhance MHC class i cross-antigen presentation by human dendritic cells," *Clin. Dev. Immunol.*, vol. 2013, 2013, doi: 10.1155/2013/362163.

[6] T. Fiolet, Y. Kherabi, C.-J. MacDonald, J. Ghosn, and N. Peiffer-Smadja, "Comparing COVID-19 vaccines for their characteristics, efficacy and effectiveness against SARS-CoV-2 and variants of concern: a narrative review.," *Clin. Microbiol. Infect. Off. Publ. Eur. Soc. Clin. Microbiol. Infect. Dis.*, vol. 28, no. 2, pp. 202–221, Feb. 2022, doi: 10.1016/j.cmi.2021.10.005.

[7] N. Doria-Rose *et al.*, "Antibody Persistence through 6 Months after the Second Dose of mRNA-1273 Vaccine for Covid-19.," *The New England journal of medicine*, vol. 384, no. 23. United States, pp. 2259–2261, Jun. 2021. doi: 10.1056/NEJMc2103916.

[8] D. H. Barouch *et al.*, "Durable Humoral and Cellular Immune Responses 8 Months after Ad26.COV2.S Vaccination.," *The New England journal of medicine*, vol. 385, no. 10. United States, pp. 951–953, Sep. 2021. doi: 10.1056/NEJMc2108829.

[9] L.-T. Yang *et al.*, "Long-lived effector/central memory T-cell responses to severe acute respiratory syndrome coronavirus (SARS-CoV) S antigen in recovered SARS patients.," *Clin. Immunol.*, vol. 120, no. 2, pp. 171–178, Aug. 2006, doi: 10.1016/j.clim.2006.05.002.

[10] L. Enjuanes, S. Zuñiga, C. Castaño-Rodriguez, J. Gutierrez-Alvarez, J. Canton, and I. Sola, "Molecular Basis of Coronavirus Virulence and Vaccine

ARTICLE IN PRESS

Development.," *Adv. Virus Res.*, vol. 96, pp. 245–286, 2016, doi: 10.1016/bs.aivir.2016.08.003.

[11] R. Channappanavar, J. Zhao, and S. Perlman, "T cell-mediated immune response to respiratory coronaviruses.," *Immunol. Res.*, vol. 59, no. 1–3, pp. 118–128, Aug. 2014, doi: 10.1007/s12026-014-8534-z.

[12] A. López-Gomez, I. Real-Arévalo, R. Martín-Palma, E. Martínez-Naves, and M. G. Del Moral, "Manufacture of Mesoporous Silicon Microparticles (MSMPs) as Adjuvants for Vaccine Delivery.," *Methods Mol. Biol.*, vol. 2673, pp. 123–130, 2023, doi: 10.1007/978-1-0716-3239-0_8.

[13] P. J. Alcolea *et al.*, "Non-replicative antibiotic resistance-free DNA vaccine encoding S and N proteins induces full protection in mice against SARS-CoV-2.," *Front. Immunol.*, vol. 13, p. 1023255, 2022, doi: 10.3389/fimmu.2022.1023255.

[14] G. Navarro-Tovar, D. Rocha-García, A. Wong-Arce, G. Palestino, and S. Rosales-Mendoza, "Mesoporous silicon particles favor the induction of long-lived humoral responses in mice to a peptide-based vaccine," *Materials (Basel).*, vol. 11, no. 7, 2018, doi: 10.3390/ma11071083.

[15] R. R. Castillo, D. Lozano, B. González, M. Manzano, I. Izquierdo-Barba, and M. Vallet-Regí, "Advances in mesoporous silica nanoparticles for targeted stimuli-responsive drug delivery: an update.," *Expert Opin. Drug Deliv.*, vol. 16, no. 4, pp. 415–439, Apr. 2019, doi: 10.1080/17425247.2019.1598375.

[16] P. L. Abbaraju *et al.*, "Asymmetric Silica Nanoparticles with Tunable Head-Tail Structures Enhance Hemocompatibility and Maturation of Immune Cells.," *J. Am. Chem. Soc.*, vol. 139, no. 18, pp. 6321–6328, May 2017, doi: 10.1021/jacs.6b12622.

[17] J. Yan, P. Siwakoti, S. Shaw, S. Bose, G. Kokil, and T. Kumeria, "Porous silicon and silica carriers for delivery of peptide therapeutics.," *Drug Deliv. Transl. Res.*, vol. 14, no. 12, pp. 3549–3567, Dec. 2024, doi: 10.1007/s13346-024-01609-7.

[18] P. L. Abbaraju, M. Jambhrunkar, Y. Yang, Y. Liu, Y. Lu, and C. Yu, "Asymmetric mesoporous silica nanoparticles as potent and safe immunoadjuvants provoke high immune responses.," *Chem. Commun. (Camb).*, vol. 54, no. 16, pp. 2020–2023, Feb. 2018, doi: 10.1039/c8cc00327k.

[19] C. A. J. Janeway, "Approaching the asymptote? Evolution and revolution in immunology.," *Cold Spring Harb. Symp. Quant. Biol.*, vol. 54 Pt 1, pp. 1–13, 1989, doi: 10.1101/sqb.1989.054.01.003.

[20] Z. Liu *et al.*, "Size effect of mesoporous silica nanoparticles on regulating the immune effect of oral influenza split vaccine.," *Colloids Surf. B. Biointerfaces*, vol. 238, p. 113920, Jun. 2024, doi: 10.1016/j.colsurfb.2024.113920.

[21] J. García-Pérez *et al.*, "Immunogenic dynamics and SARS-CoV-2 variant neutralisation of the heterologous ChAdOx1-S/BNT162b2 vaccination: Secondary analysis of the randomised CombiVacS study.," *EClinicalMedicine*, vol. 50, p. 101529, Aug. 2022, doi: 10.1016/j.eclinm.2022.101529.

[22] Q. Lin, L. Zhu, Z. Ni, H. Meng, and L. You, "Duration of serum neutralizing antibodies for SARS-CoV-2: Lessons from SARS-CoV infection.," *Journal of microbiology, immunology, and infection = Wei mian yu gan ran za zhi*, vol. 53, no. 5. England, pp. 821–822, Oct. 2020. doi: 10.1016/j.jmii.2020.03.015.

[23] A. Flaxman *et al.*, "Reactogenicity and immunogenicity after a late second dose or a third dose of ChAdOx1 nCoV-19 in the UK: a substudy of two randomised controlled trials (COV001 and COV002).," *Lancet (London, England)*, vol. 398, no. 10304, pp. 981–990, Sep. 2021, doi: 10.1016/S0140-

ARTICLE IN PRESS

6736(21)01699-8.

[24] S. Nazeri, S. Zakeri, A. A. Mehrizi, S. Sardari, and N. D. Djadid, “Measuring of IgG2c isotype instead of IgG2a in immunized C57BL/6 mice with Plasmodium vivax TRAP as a subunit vaccine candidate in order to correct interpretation of Th1 versus Th2 immune response,” *Exp. Parasitol.*, vol. 216, Sep. 2020, doi: 10.1016/J.EXPPARA.2020.107944.

[25] A. Adam *et al.*, “A modified porous silicon microparticle potentiates protective systemic and mucosal immunity for SARS-CoV-2 subunit vaccine.,” *Transl. Res.*, vol. 249, pp. 13–27, Nov. 2022, doi: 10.1016/j.trsl.2022.06.004.

[26] C. O. Barnes *et al.*, “SARS-CoV-2 neutralizing antibody structures inform therapeutic strategies,” *Nature*, vol. 588, no. 7839, p. 682, Dec. 2020, doi: 10.1038/S41586-020-2852-1.

[27] H. Li *et al.*, “The Abundant Distribution and Duplication of SARS-CoV-2 in the Cerebrum and Lungs Promote a High Mortality Rate in Transgenic hACE2-C57 Mice.,” *Int. J. Mol. Sci.*, vol. 25, no. 2, Jan. 2024, doi: 10.3390/ijms25020997.

[28] T. N. Starr *et al.*, “Deep Mutational Scanning of SARS-CoV-2 Receptor Binding Domain Reveals Constraints on Folding and ACE2 Binding,” *Cell*, vol. 182, no. 5, pp. 1295-1310.e20, Sep. 2020, doi: 10.1016/J.CELL.2020.08.012.

[29] H. Liu *et al.*, “The basis of a more contagious 501Y.V1 variant of SARS-CoV-2,” *Cell Res.*, vol. 31, no. 6, pp. 720–722, Jun. 2021, doi: 10.1038/S41422-021-00496-8.

[30] J. García-Arriaza *et al.*, “COVID-19 Vaccine Candidates Based on Modified Vaccinia Virus Ankara Expressing the SARS-CoV-2 Spike Protein Induce Robust T- and B-Cell Immune Responses and Full Efficacy in Mice,” *J. Virol.*, vol. 95, no. 7, Mar. 2021, doi: 10.1128/JVI.02260-20.

[31] P. He, Y. Zou, and Z. Hu, “Advances in aluminum hydroxide-based adjuvant research and its mechanism,” *Hum. Vaccin. Immunother.*, vol. 11, no. 2, p. 477, 2015, doi: 10.1080/21645515.2014.1004026.

[32] S. A. Hudu, S. H. Shinkafi, and S. Umar, “An overview of recombinant vaccine technology, adjuvants and vaccine delivery methods,” *Int. J. Pharm. Pharm. Sci.*, vol. 8, no. 11, pp. 19–24, 2016, doi: 10.22159/ijpps.2016v8i11.14311.

ARTICLE IN PRESS

Author Contributions statement:

All authors contributed to the study conception and design. Material preparation, data collection and analysis were performed by A.L-G., I.R-A., E.M-H., J.A.C., D.L-F., P. N-A., B R-P., B. A-P., B. M-A. and I. J. The first draft of the manuscript was written by M. G. M., E.M.N., and A. L-G. N.S., A. M-del-P. and R. J. M-P. commented on previous versions of the manuscript. All authors read and approved the final manuscript.

Competing interests statements:

ARTICLE IN PRESS

The authors declare that no funds, grants, or other support were received during the preparation of this manuscript. The authors have no relevant financial or non-financial interests to disclose.

Ethics Approval:

This study was performed in line with the principles of the Declaration of Helsinki. Approval was granted by the Ethics Committee of Universidad Complutense of Madrid and Comunidad of Madrid (Dec 14/2022/ PROEX 272.5/22).

Consent to participate:

Informed consent was obtained from all individual participants included in the study.

Conflict of interest:

The authors declare that the research was conducted in the absence of any commercial or financial relationships that could be construed as a potential conflict of interest.

ARTICLE IN PRESS